Pre-Clinical Research Report

Journal of INTERNATIONAL MEDICAL RESEARCH

Journal of International Medical Research
2018, Vol. 46(6) 2371–2385

DOI: 10.1177/0300060518762060
journals.sagepub.com/home/imr
SAGE

Icariin influences cardiac remodeling following myocardial infarction by regulating the CD147/MMP-9 pathway

Yu Shi[1,#], Weihong Yan[1,#], Qiaoyan Lin[1] and Weimin Wang[2]

Abstract

Objective: We investigated the protective effect of icariin on myocardial infarction-induced cardiac remodeling.

Methods: A cardiac remodeling model was constructed by ligating rats' coronary artery. Different icariin and CD147 concentrations were administered in the model group, and echocardiography was used to detect systolic function, screening out ideal experimental concentrations. The ventricular systolic function, myocardial apoptosis rate, and expression of collagen type I (Col I), Col III, CD147, matrix metalloproteinase 9 (MMP-9), and tissue inhibitor of metalloproteinase 1 (TIMP-1) were detected by hematoxylin–eosin staining, TUNEL assay, and western blot. MMP-9 activity was evaluated by gelatin zymography.

Results: The expression of Col I, Col III, CD147, and MMP-9 was higher, the expression of TIMP-1 was lower, and the maximal rates of left ventricular pressure rise and fall ($+dp/dt_{max}$ and $-dp/dt_{max}$, respectively) were lower in model than control rats. The expression of CD147, MMP-9, Col I, and Col III was lower, the expression of TIMP-1 was higher, and the $+dp/dt_{max}$ and $-dp/dt_{max}$ were higher in the icariin than model group. The apoptosis rate was lower in the icariin and icariin + CD147 groups than control group.

Conclusion: Icariin attenuated myocardial apoptosis following myocardial infarction by apoptosis rate reduction and CD147/MMP-9 pathway inhibition.

[1]Department of Cardiology, the Affiliated Yantai Yuhuangding Hospital of Qingdao University, Yantai, Shandong, China
[2]Department of Electrocardiogram, the Affiliated Yantai Yuhuangding Hospital of Qingdao University, Yantai, Shandong, China

[#]These authors contributed equally to this work.

Corresponding author:
Weimin Wang, Department of Electrocardiogram, the Affiliated Yantai Yuhuangding Hospital of Qingdao University, No. 20 East Yuhuangding Road, Zhifu District, Yantai, Shandong 264001, China.
Email: azhangh100@126.com

Keywords
Myocardial infarction, cardiac remodeling, icariin, CD147/MMP-9 pathway, collagen, apoptosis

Date received: 10 November 2017; accepted: 7 February 2018

Introduction

In recent years, the morbidity and mortality rates associated with coronary heart disease have increased; in particular, the rates of death and disability associated with acute myocardial infarction (AMI) have been the highest.[1] AMI mainly refers to partial myocardial ischemia, hypoxia, and necrosis caused by acute coronary occlusion and blood flow occlusion. AMI is currently the focus of treatment for cardiac arrest.[2] An in-depth study showed that a large area of myocardial infarction (MI) could lead to cardiac remodeling. Cardiac remodeling following AMI refers to the changes in the ventricular morphology and structures caused by mechanical stress, endocrine stimulation, and cytokine activation. These changes are characterized by thinning, stretching, or bulging of the wall in the infarct region with reactive hypertrophy and lengthening of the wall in the non-infarct region, resulting in advanced ventricular dilatation. Cardiac remodeling is closely associated with the development and progression of AMI in patients with heart failure and should therefore be given close attention.[3] CD147 is a transmembrane glycoprotein that can induce a variety of cells to express matrix metalloproteinases (MMPs). Previous studies have shown that the CD147/MMP pathway is closely associated with neoplastic metastasis, atherosclerosis, and embryo implantation.[4] Under the function of zinc ions, MMP-9 is involved in the degradation and reconstruction of extracellular mechanisms.[5] MMPs are also highly expressed in early MI[6]; thus, regulation of the CD147/MMP-9 pathway in the process of cardiac remodeling following MI is of great importance. *Epimedium* spp. have been commonly used in traditional Chinese medicine as a pharmaceutical treatment for osteoporosis. Studies have shown that icariin, the main component of *Epimedium* spp., has an inhibitive effect on the expression of MMP-9 in osteoclasts of mice; however, its signaling mechanisms have not been studied specifically.[7] Further studies have shown that icariin has a protective effect on myocardial ischemia-reperfusion injury,[8] but there is a lack of studies on the relationship between icariin and cardiac remodeling following MI. The present study was performed to investigate the influence of icariin on the CD147/MMP-9 pathway in cardiac remodeling following MI in rats.

Materials and methods

Main drugs, reagents, and instruments

The two drugs used in this study were icariin (Sigma-Aldrich, St. Louis, MO, USA) and CD147 protein (Sino Biological Inc., Beijing, China).

The reagents used were RNA extraction and polymerase chain reaction (PCR) primers and reagents (Invitrogen Inc., Carlsbad, CA, USA), TUNEL antibody (Abcam Inc., Cambridge, MA, USA), Bax, Bcl-2, active caspase-3, collagen types I/III (Col I/III), CD147, MMP-9, tissue inhibitor of metalloproteinase 1 (TIMP-1),

β-actin and other antibodies (Abcam Inc.), bicinchoninic acid, and quantitative western blot reagent.

Finally, the instruments used were a VEVO2100 small animal ultrasound imaging system (VisualSonics Inc., Toronto, Canada), P3 Plus multi-channel polygraph (Ponemah Physiology Platform, Valley View, OH, USA), microscope (Olympus Optical Co., Ltd., Tokyo, Japan), microplate reader (BioTek Instruments, Inc., Winooski, VT, USA), PCR instrument (Thermo Fisher Scientific, San Jose, CA, USA), low-speed centrifuge (Beckman Coulter, Fullerton, CA, USA), and Gel Doc XR+ imaging system (Bio-Rad Laboratories, Hercules, CA, USA).

Construction of cardiac remodeling model

One hundred male Sprague–Dawley rats (age, 7–8 weeks; weight, 220–250 g) were provided by Qingdao University. All procedures in this experiment were approved by the Institutional Medical Experimental Animal Care Committee of Qingdao University and the ethics committee of the Affiliated Yantai Yuhuangding Hospital of Qingdao University. The cardiac remodeling model following MI was prepared by ligation of the coronary artery in rats for 4 weeks. After anesthesia with 3% sodium pentobarbital (35 mg/kg) and thoracotomy, the coronary artery was ligated about 4 mm from the lower edge of the left atrial appendage. The procedures in the sham operation group were the same as those in the AMI model group, but the suture that was passed through the coronary artery was not ligated, and the chest was quickly closed. After 24 hours, the rats in the sham operation and model groups underwent electrocardiographic examinations. The ST-segment was elevated to >0.2 mV and continued for 30 minutes, which was considered as a successful operation standard. The rats in the control group were treated without surgery.

Screening for appropriate concentrations of icariin and CD147

At 24 hours after surgery, five rats in the sham operation group were randomly selected to undergo intraperitoneal injection of 2 mL/kg per day of saline. The 25 rats in the model group were divided into 5 groups of 5 rats each: injection of 2 mL/kg per day of saline, injection of different concentrations of icariin solution (Sigma-Aldrich) at dosages of 3, 6, 12, and 20 mg/kg per day dissolved in the same amount of saline. Rats in the control group were injected with 2 mL/kg per day of saline. At 28 days after surgery, the rats in each group underwent echocardiographic examinations. After the rats were anesthetized, the fur at the left junction of the chest and abdomen was removed with depilatory paste. Under spontaneous breathing, the left ventricular end-diastolic dimension (LVDd), left ventricular end-systolic diameter (LVDs), and end-diastolic left ventricular anterior wall thickness (LVAWd) were measured at the papillary level. Through the left ventricular long-axis view, the left ventricular end-diastolic volume and left ventricular end-systolic volume were measured by the single-plane area-length method, and the left ventricular ejection fraction (LVEF) was then calculated. All indicators were averaged after the measurement of three consecutive cardiac cycles, screening for the optimum concentration of icariin. Next, 15 rats from the model group were randomly selected and divided into 3 groups of 5 rats each. The rats in each group were intravenously injected with 5, 10, and 15 mg/kg per day of soluble CD147 (Sino Biological Inc.), followed by intraperitoneal injection with the optimum concentration of icariin. After 28 days, the rats in each group underwent echocardiographic examinations to screen

for the optimum concentration of CD147. The above-mentioned indexes were also analyzed.

Hemodynamic changes in rats

At 24 hours after surgery, 10 rats in the control group, 10 rats in the sham operation group, and 30 rats in the model group were randomly selected. The rats in the model group were randomly divided into 3 groups of 10 rats each and injected with 2 mL/kg per day of physiological saline, 12 mg/kg per day of icariin (Sigma-Aldrich), and 12 mg/kg per day of icariin + 10 mg/kg per day of CD147 (Sino Biological Inc.), respectively. In the sham operation and control groups, the rats were injected with 2 mL/kg per day of saline until 28 days postoperatively. The rats were fasted for 24 hours before being anesthetized, after which the right common carotid artery was isolated. A plastic pipe (1-mm internal diameter) was inserted into the left ventricle and connected to a P3 Plus multichannel polygraph (Ponemah Physiology Platform). After the plastic pipe had stabilized for 20 minutes, the left ventricular end-diastolic pressure (LVEDP) and maximal rate of left ventricular pressure rise and fall ($+dp/dt_{max}$ and $-dp/dt_{max}$, respectively) were recorded. The common carotid artery was isolated, the heart rate (HR) was measured by intubation, and the mean arterial pressure (MAP) was recorded.

Myocardial morphological changes and myocardial cell apoptosis in rats

The rats were sacrificed and fixed in the supine position, and their chest was opened along the xiphoid to both axillae. The heart was removed and placed in cold phosphate-buffered saline (PBS) to wash away the residual liquid with filter paper. The rats were then weighed with a 1/10,000 analytical balance. Part of the left ventricle was cut and fixed with 4% paraformaldehyde for 18 to 24 hours. The ratio of the heart weight (HW) and body weight (BW) was calculated using the following formula: HW/BW ratio = (HW / BW) × 100%. Next, the tissue was removed from the fixative and dehydrated with gradient concentrations of alcohol in the following order: 70% ethanol (1 hour), 80% ethanol (1 hour), 95% ethanol (two times at 1 hour each), and 100% ethanol (three times at 0.5 hours, 0.5 hours, and 1 hour, respectively). The tissue was then treated with xylene immersion (two times at 1 hour each), paraffin-embedded at 65°C for 3 to 4 hours, cut into slices with a thickness of 3 to 4 μm, and mounted on a slide for the follow-up experiments. The paraffin sections were dewaxed in xylene, washed by alcohol with graded concentrations to clean the hydrate, stained with hematoxylin for 10 to 15 minutes, and washed with water. After 1% hydrochloric acid–alcohol differentiation for 30 seconds, the paraffin sections were washed with water, blued with saturated lithium for 3 minutes, washed with running water for 15 to 30 minutes, disseminated with 1% alcohol-soluble eosin for 5 to 15 seconds, and finally processed by conventional dehydration and mounting. The morphological changes in the myocardial tissues were observed under a microscope (Olympus Optical Co., Ltd.). The surface area of the cells was carefully observed. Taking the control group as 1 for reference, the area of the cells in the other groups was calculated as the ratio of the area of myocardial cells to the area of the myocardial cells in the control group. Paraffin sections were dried at 60°C for 1 hour before hydration, placed into 0.01 mol/L citric acid buffer, heated in a microwave for 10 minutes for antigen retrieval, and incubated with 0.3% Triton-X100 for 30 minutes. The sections were then washed with running water for 5 minutes

and washed three times with PBS (5 minutes each time). The excess moisture around the tissue was dried, and 50 μL of TUNEL reaction mixture (Abcam Inc.) was added dropwise (treatment group, 50 μL of TdT mixed with 450 μL of fluorescein-labeled dUTP; negative control group, only 50 μL of fluorescein-labeled dUTP; and positive control group, 100 μL of DNase I was added at 25°C and reacted for 10 minutes, followed by the same procedures performed in the treatment group). The sections were placed in a dark moist chamber at 37°C for 1 hour, rinsed with PBS three times for 5 minutes each, incubated in phalloidin (1:50 dilution) for 1 hour, rinsed with PBS three times for 5 minutes each, and finally mounted with 4′,6-diamidino-2-phenylindole-containing anti-quenching reagent. Green fluorescence particles observed under the microscope were apoptotic myocardial cells. Five fields of view were randomly selected at 200× magnification to count the number of apoptotic nuclei and total number of myocardial cells. The myocardial cell apoptosis index was calculated (apoptosis rate = number of apoptotic cells / total number of cardiomyocytes). To obtain more accurate results, the experiment was repeated three times and the average value was calculated.

Expression levels of Bax, Bcl-2, caspase-3, and Col I/III in myocardial tissues

In total, 30 mg of myocardial tissues were minced with scissors and placed into a 2-mL Eppendorf tube. According to the instructions for the Trizol™ kit, the total RNA was extracted and the RNA concentration and purity were determined. Total RNA (1 μg) was selected and reverse-transcribed into cDNA. The cDNA (5 μL) was obtained and diluted four-fold, 2 μL of which was used as a template, and quantitative PCR was conducted using the primers of the target genes and reference glyceraldehyde 3-phosphate dehydrogenase (GAPDH). The reaction conditions were as follows: pre-denaturation for 3 s at 95°C, denaturation for 10 s at 95°C, and annealing/extension for 30 s at 60°C; this was repeated for 40 cycles. The plate was read with a temperature increase of 0.5°C every 5 s from 65°C to 95°C to draw the dissolution curve. All samples were provided with three parallel tubes, and the gene expression level was represented by average threshold cycle value (Ct). The $2^{-\Delta\Delta Ct}$ method was used to calculate the relative expression levels of Bcl-2, Bax, caspase-3, Col I, and Col III. For western blotting, 30 mg of myocardial tissue was minced with scissors and placed into a 2-mL Eppendorf tube. Next, 60 μL of 2% sodium dodecyl sulfate (SDS) protein lysate (pre-added phosphatase inhibitor) was added and the mixture was fully homogenized until no tissue residue was present (operation on ice). The tube was centrifuged at 14,000 rpm for 10 minutes at 4°C using a low-speed centrifuge (Beckman Coulter) and stored at −80°C. After measurement of the protein concentration by bicinchoninic acid reagent (Invitrogen Inc.), each 30 μg of protein was fractionated by polyacrylamide gel electrophoresis (PAGE) and transferred to a membrane for 60 to 90 minutes under 100 V constant voltage. The membrane was then sealed for 1 to 2 hours with 5% skim milk/tris-buffered saline (TBS) with 0.1% Tween 20 (TBST) at room temperature. Next, 1:1000 Bcl-2/Bax/active caspase-3 antibodies and 1:800 Col I/III antibodies were added, and the membrane was incubated overnight at 4°C. As a reference, 1:5000 β-actin was incubated at room temperature for 1.5 hours. The TBST membrane was cleaned three times for 10 minutes each. It was then incubated at room temperature with horseradish peroxidase-labeled goat anti-rabbit/anti-mouse secondary antibody for 2 hours. Next, the TBST membrane was cleaned twice for 10 minutes each,

and the TBS membrane was cleaned for 5 minutes. After electrochemiluminescence detection and color development, image formation was performed using the Gel Doc XR+ imaging system (Bio-Rad Laboratories), and the ratio of each band's euphotic volume was recorded. The relative expression quantity of the target protein β-actin served as the internal reference band. All sequences of the primers used for PCR are shown in Table 1. This experiment was repeated three times.

Expression levels of CD147, MMP-9, and TIMP-1 in myocardial tissues

According to the above-described steps in the subsection titled "Myocardial morphological changes and myocardial cell apoptosis in rats," quantitative PCR (Thermo Fisher Scientific) and western blot reagent (Invitrogen Inc.) were used to detect myocardial tissue CD147 (antibody 1:1000), the mRNA and protein expression of MMP-9 (antibody 1:1000), and TIMP-1 (antibody 1:1000). Gelatin zymography was used to detect MMP-9 activity (Zymogram Gels; Thermo Fisher Scientific) according to the manufacturer's protocol. Briefly, protein was extracted from frozen samples containing 10 mg of protein and mixed with 10 mL of sample buffer, then subjected to SDS-PAGE in 5% polyacrylamide gels that were copolymerized with 2 mg/mL of gelatin at 4°C for 1 hour. After electrophoresis, the gels were washed twice in the rinsing buffer for 1 hour at room temperature to remove SDS. They were then incubated for 36 hours at 37°C in the incubation buffer. The gels were stained with 0.1% Coomassie Brilliant Blue R-250 for 30 minutes and destained for 8 hours in a solution of 10% acetic acid and 10% isopropanol. The proteolytic activity was shown as clear bands against the blue background of stained gelatin. The experiment was repeated three times.

Table 1. Sequences of PCR primers of detected genes

Genes	Primer	Sequence (5′–3′)
Bax	Forward	AGACAGGGGCCTTTTTGCTAC
	Reverse	AATTCGCCGGAGACACTCG
Bcl-2	Forward	GCTACCGTCGTGACTTCGC
	Reverse	CCCCACCGAACTCAAAGAAGG
Caspase-3	Forward	CTCGCTCTGGTACGGATGTG
	Reverse	TCCCATAAATGACCCCTTCATCA
Col I	Forward	GCTCCTCTTAGGGGCCACT
	Reverse	ATTGGGGACCCTTAGGCCAT
Col III	Forward	CTGTAACATGGAAACTGGGGAAA
	Reverse	CCATAGCTGAACTGAAAACCACC
CD147	Forward	GTGGCGTTGACATCGTTGG
	Reverse	CTATGTACTTCGTATGCAGGTCG
MMP-9	Forward	GCAGAGGCATACTTGTACCG
	Reverse	TGATGTTATGATGGTCCCACTTG
TIMP-1	Forward	CGAGACCACCTTATACCAGCG
	Reverse	ATGACTGGGGTGTAGGCGTA
GAPDH	Forward	AGGTCGGTGTGAACGGATTTG
	Reverse	GGGGTCGTTGATGGCAACA

PCR, polymerase chain reaction; Col I, collagen type I; Col III, collagen type III; MMP-9, matrix metalloproteinase 9; TIMP-1, tissue inhibitor of metalloproteinase 1; GAPDH, glyceraldehyde 3-phosphate dehydrogenase.

Statistical analysis

IBM SPSS Statistics, version 19.0 (IBM Corp., Armonk, NY, USA) was used to perform t tests or one-way analysis of variance to analyze the measurement data. All data are presented as mean ± standard deviation. A P value of <0.05 was considered statistically significant.

Results

Electrocardiographic changes of rats in each group

In the sham group, the P-wave sequence of the rats occurred with a regular rhythm, and the QRS wave, T-wave, and ST-segment were normal. In the model group, the ST-segment of the rats was elevated after surgery, proving that the establishment of the animal models was successful (Figure 1(a)).

Screening for concentrations of icariin and CD147

As shown in Table 2, LVDd and LVDs were significantly higher ($P < 0.05$) while LVAWd and LVEF were significantly lower ($P < 0.05$) in the model groups than in the control group, which was of statistical significance for the rats receiving different

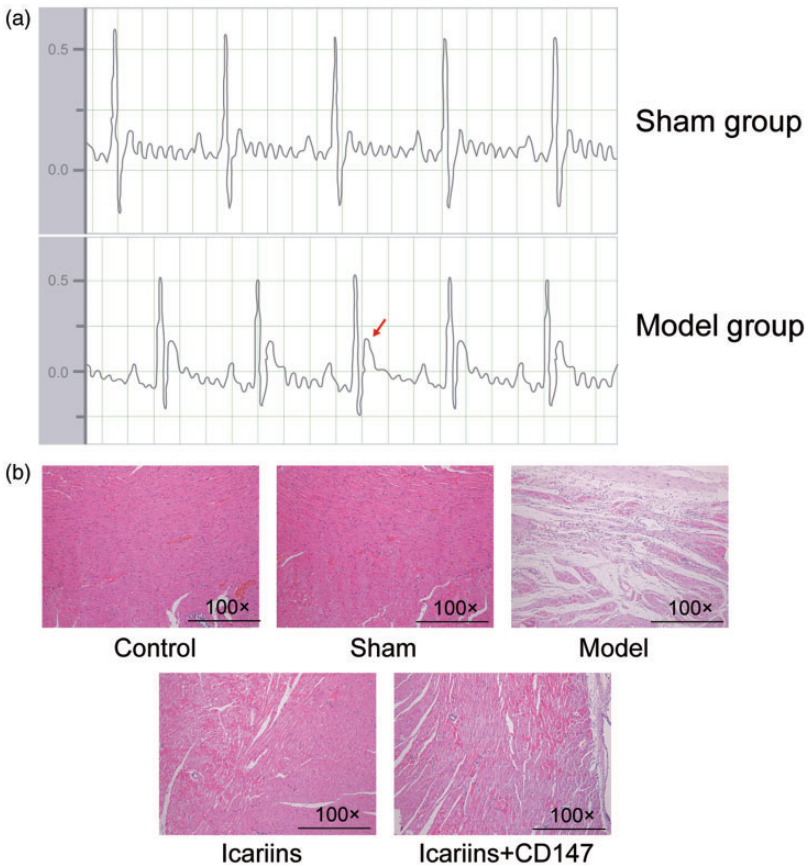

Figure 1. (a) Electrocardiograms of rats in the sham and model groups. (b) Hematoxylin–eosin staining of the rats' heart tissues in different groups. Scale bar = 100 μm.

Table 2. Hemodynamic changes after treatment with various dosages of icariin

	LVDd (cm)	LVDs (cm)	LVAWd (cm)	LVEF (%)
Group				
Control	0.49 ± 0.04	0.25 ± 0.02	0.15 ± 0.03	79.12 ± 2.84
Sham	0.50 ± 0.05	0.24 ± 0.03	0.15 ± 0.02	78.86 ± 4.13
Model (dosage of icariin; mg/kg per day)				
0	0.68 ± 0.12*	0.49 ± 0.11*	0.09 ± 0.02*	48.86 ± 3.79*
3	0.62 ± 0.15*	0.46 ± 0.05*	0.11 ± 0.03*	51.14 ± 4.42*
6	0.57 ± 0.08*#	0.37 ± 0.08*#	0.12 ± 0.02*#	62.81 ± 2.88*#
12	0.53 ± 0.05*#	0.30 ± 0.05*#	0.14 ± 0.03#	72.12 ± 4.12*#
20	0.53 ± 0.06*#	0.29 ± 0.06*#	0.14 ± 0.11#	74.01 ± 5.81*#

Data are presented as mean ± standard deviation.
LVDd, left ventricular end-diastolic dimension; LVDs, left ventricular end-systolic diameter; LVAWd, end-diastolic left ventricular anterior wall thickness; LVEF, left ventricular ejection fraction.
*$P < 0.05$ compared with control group; #$P < 0.05$ compared with model group (0 mg/kg per day). n = 3.

Table 3. Hemodynamic changes after treatment with various dosages of CD147

Dosage of CD147 (mg/kg per day)	LVDd (cm)	LVDs (cm)	LVAWd (cm)	LVEF (%)
5	0.61 ± 0.04	0.35 ± 0.04	0.12 ± 0.03	65.11 ± 4.17
10	0.67 ± 0.05Δ	0.48 ± 0.05*	0.09 ± 0.02*	51.12 ± 3.14*
15	0.68 ± 0.05Δ	0.51 ± 0.06*	0.09 ± 0.01*	50.09 ± 2.88*

Data are presented as mean ± standard deviation.
LVDd, left ventricular end-diastolic dimension; LVDs, left ventricular end-systolic diameter; LVAWd, end-diastolic left ventricular anterior wall thickness; LVEF, left ventricular ejection fraction.
*$P < 0.05$ compared with model rats treated with 5 mg/kg per day of CD147. n = 3.

concentrations of icariin. There were no significant differences in LVDd, LVDs, LVAWd, or LVEF between rats treated with 12 and 20 mg/kg per day of icariin. As shown in Table 3, the LVDd and LVDs were significantly higher ($P < 0.05$) while the LVEF and LVAWd were significantly lower ($P < 0.05$) in rats treated with 10 and 15 mg/kg per day of CD147 than in rats treated with 5 mg/kg per day of CD147. There was no significant difference in the above indexes between rats treated with 10 and 15 mg/kg per day of CD147.

Hemodynamic changes of rats in each group

The MAP and the $+dp/dt_{max}$ and $-dp/dt_{max}$ were significantly lower while the HR and LVEDP were significantly higher in the model group and icariin + CD147 groups than in the control group ($P < 0.05$ for all) (Table 4). There were no significant differences in the HR, MAP, $+dp/dt_{max}$, or $-dp/dt_{max}$ between the icariin and control groups, while the HR was significantly higher in the icariin group ($P < 0.05$). The MAP, LVEDP, $+dp/dt_{max}$, and $-dp/dt_{max}$ were markedly different between the icariin group and icariin + CD147 group ($P < 0.05$), indicating that CD147 neutralized the effect of icariin in rats in the model group.

Myocardial morphological changes of rats in each group

The HW/BW ratio was significantly higher in the model, icariin, and icariin + CD147

Table 4. Hemodynamic changes of rats among different groups

Group	HR (beats per minute)	MAP (mmHg)	LVEDP (mmHg)	$+dp/dt_{max}$ (mmHg/s)	$-dp/dt_{max}$ (mmHg/s)
Control	441.0 ± 35.5	115.2 ± 11.7	5.8 ± 1.2	4481.5 ± 279.4	167.9 ± 11.2
Sham	451.7 ± 51.4	117.5 ± 10.8	5.9 ± 1.4	4417.6 ± 208.5	165.4 ± 10.8
Model	520.9 ± 74.3*	91.0 ± 7.2*	25.1 ± 5.2*	3519.5 ± 115.6*	131.8 ± 7.5*
Icariin	455.9 ± 34.8#	106.9 ± 8.5#	10.2 ± 3.1*#	4275.8 ± 194.2#	171.9 ± 12.5#
Icariin + CD147	511.2 ± 47.5*#Δ	96.5 ± 7.4*#Δ	17.5 ± 4.1*#Δ	3961.8 ± 127.4*#Δ	152.1 ± 11.0*#Δ

Data are presented as mean ± standard deviation.
HR, heart rate; MAP, mean arterial pressure; LVEDP, left ventricular end-diastolic pressure; $+dp/dt_{max}$, maximal rate of left ventricular pressure rise; $-dp/dt_{max}$, maximal rate of left ventricular pressure fall.
*$P < 0.05$ compared with control group; #$P < 0.05$ compared with model group; Δ$P < 0.05$ compared with icariin group. n = 3.

Table 5. HW/BW ratio and myocardial apoptosis rate changes among different groups

Group	HW/BW ratio (mg/g)	Apoptosis rate (%)
Control	6.17 ± 0.09	0.00 ± 0.00
Sham	6.20 ± 0.11	0.05 ± 0.03
Model	7.02 ± 0.14*	17.81 ± 4.12*
Icariin	6.37 ± 0.12*#	4.75 ± 0.67*#
Icariin + CD147	6.89 ± 0.15*#Δ	5.12 ± 0.54*#Δ

Data are presented as mean ± standard deviation.
HW, heart weight; BW, body weight.
*$P < 0.05$ compared with control group; #$P < 0.05$ compared with model group; Δ$P < 0.05$ compared with icariin group. n = 3.

groups than in the control group ($P < 0.05$) (Table 5). The HW/BW ratio was significantly lower in the icariin and icariin + CD147 groups than in the model group ($P < 0.05$). Furthermore, the HW/BW ratio in the icariin + CD147 group fell between that in the model and icariin groups ($P < 0.05$). In addition, the morphological changes of myocardial cells were observed using hematoxylin–eosin staining. As illustrated in Figure 1(b), in both the control and sham operation groups, the cardiac histiocytes were well organized with consistent shapes of fibers and clear cardiomyocytic nuclei. In the model group, the fibroblasts, endothelial cells, and intercellular substance in the infarction region were increased, forming a scar area. In addition, the normal cells had transformed to a disorderly growth pattern. In the icariin group, a disordered arrangement of myocardial cells was still present in the infarction region with a smaller scar area. In the icariin + CD147 group, myocardial cells were occasionally present in this region, and more fibroblasts were present with a disordered arrangement.

Apoptosis level of myocardial cells in each group

Correspondingly, the apoptosis rates showed a trend similar to the HW/BW ratio among the groups. The apoptosis rate of cells and the expression levels of Bax, caspase-3, and cleaved caspase-3 were significantly higher in the model, icariin, and icariin + CD147 groups than in the control group ($P < 0.05$ for all) (Table 5, Figure 2), while the expression level of Bcl-2 was significantly lower ($P < 0.05$) (Figure 2). In addition, the apoptosis rate of myocardial cells and expression levels of Bax, caspase-3, and cleaved caspase-3 were lower in the icariin and icariin + CD147 groups than in the model group ($P < 0.05$), while the expression level of Bcl-2 was higher ($P < 0.05$).

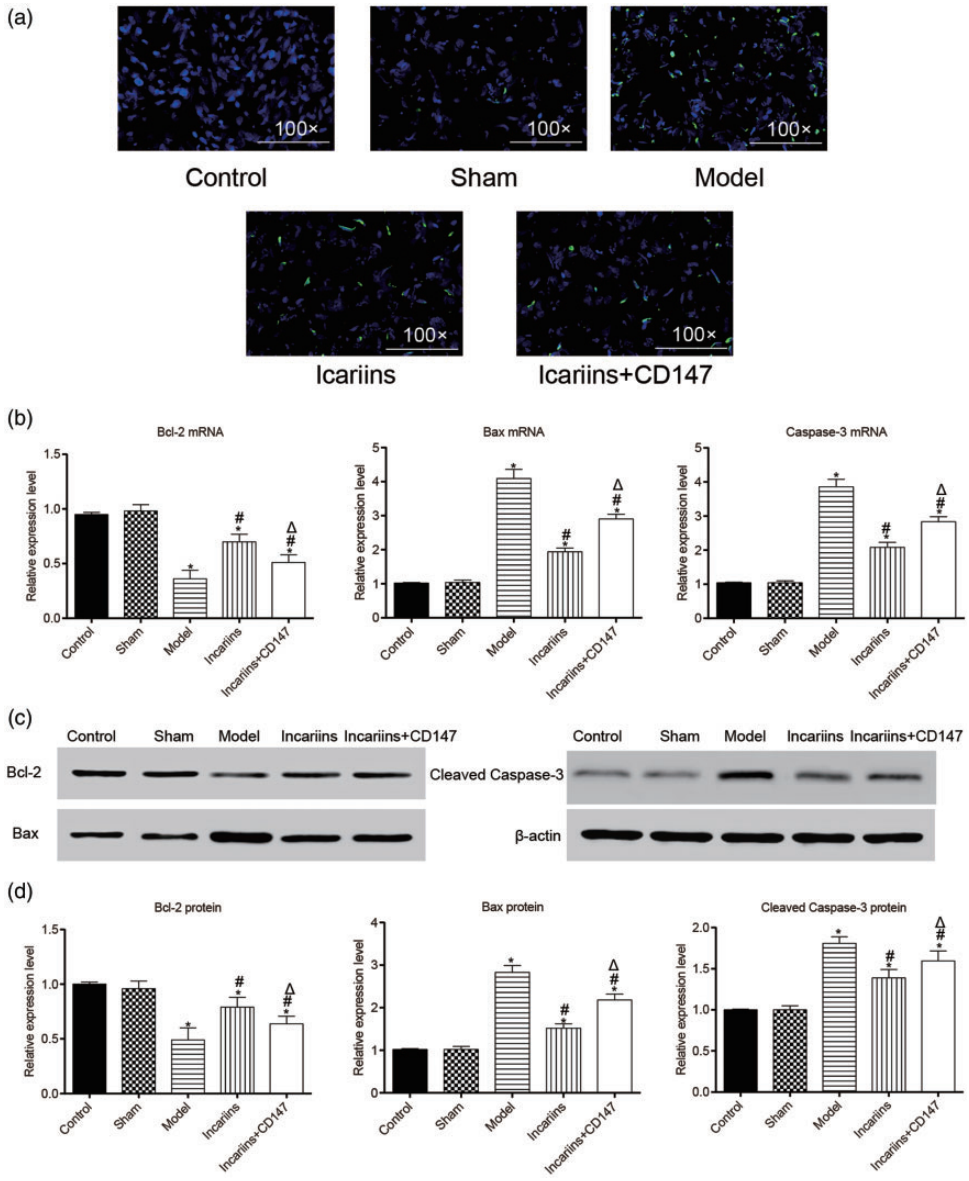

Figure 2. Apoptosis rate and expression levels of Bcl-2, Bax, and caspase-3 in rat hearts in different groups. (a) TUNEL staining of rats' heart tissues in different groups; Scale bar = 200 μm. (b) mRNA expression levels. (c, d) Protein expression levels. *$P < 0.05$ compared with the control group; #$P < 0.05$ compared with the model group; Δ$P < 0.05$ compared with the icariin group. n = 3.

Expression levels of Col I/III in myocardial tissues of rats in each group

The expression levels of Col I/III in the model, icariin, and icariin + CD147 groups were significantly higher than those in the control group ($P < 0.05$) (Figure 3). The expression levels of Col I/III were significantly lower in the icariin group than in

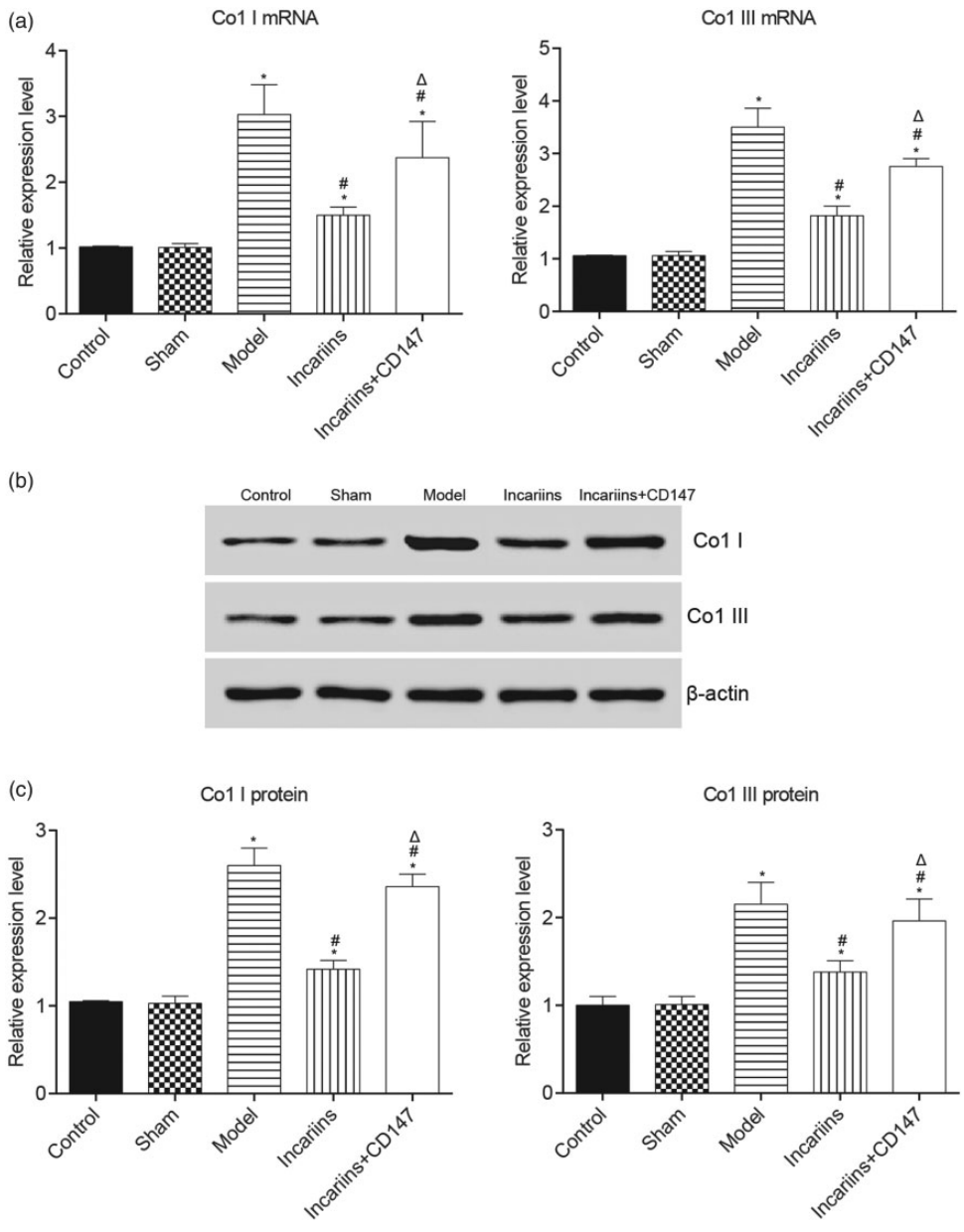

Figure 3. Expression levels of Col I and Col III of rat hearts in different groups. (a) mRNA expression levels. (b, c) Protein expression levels. $*P < 0.05$ compared with the control group; $\#P < 0.05$ compared with the model group; $\Delta P < 0.05$ compared with the icariin group. n = 3. Col I, collagen type I; Col III, collagen type III.

the model and icariin + CD147 groups ($P < 0.05$). The expression levels of Col I/III were also significantly different between the icariin + CD147 group and icariin group ($P < 0.05$), indicating that CD147 reversed the influence of icariin and intensified cardiac remodeling following MI.

Expression levels of CD147, MMP-9, and TIMP-1 in myocardial tissues of rats in each group

The expression levels of CD147 and MMP-9 and the MMP-9 activity were significantly higher in the model group than in the control group ($P < 0.05$) (Figure 4), while the expression level of TIMP-1 was significantly lower ($P < 0.05$). The expression level of CD147 was significantly lower in the icariin and icariin + CD147 groups than in the model group ($P < 0.05$). There was also a significant difference in the expression levels of MMP-9 and TIMP-1 between the two above groups ($P < 0.05$), whereas no difference was observed in CD147.

Discussion

Cardiac remodeling is an important pathophysiological mechanism affecting the cardiac function and prognosis of patients with AMI. Changes in the ventricular volume, shape, wall thickness, cardiac structure, and quantity of collagen fibers following MI will result in gradual cardiomyocyte hypertrophy, interstitial fibrosis, and cardiac enlargement with subsequent cardiac remodeling and ultimately heart failure.[9] In the present study, we successfully constructed a model of MI-induced cardiac remodeling by ligating the coronary artery of rats[10] and found significant ventricular wall thinning, heart chamber expansion, and a decreased LVEF in the rats of the model group, which are common outcomes of cardiac remodeling. Different concentrations of icariin inhibited the cardiac remodeling of rats in a dose-dependent manner, but there was no significant difference in the LVDd, LVDs, LVAWd, or LVEF between dosages of 20 and 12 mg/kg per day of icariin. In rats given 12 mg/kg per day of icariin and injected with different concentrations of CD147, the LVDd and LVDs were significantly higher while the LVAWd and LVEF were lower at CD147 dosages of 10 and 15 mg/kg per day than 5 mg/kg per day, indicating that CD147 may be associated with the progression of cardiac remodeling following MI.

The CD147 molecule is a transmembrane glycoprotein widely expressed in a variety of human tissues and cells. It belongs to the immunoglobulin superfamily, the main biological activity of which is to induce MMPs.[11] MMPs can degrade all extracellular matrix components of cells in addition to polysaccharides. MMPs in myocardial tissues can degrade the myocardial matrix, and at higher activities, MMPs can increase the degradation of collagenous fibers.[12] MMP-9 has a regulatory role in collagen synthesis. Higher MMP activity is often associated with increased collagen.[13] The most prominent structural change induced by AMI in the present study was left ventricular dilatation as well as loss and remodeling of the extracellular matrix during MI, which is a key factor of cardiac remodeling. The expression levels of Col I/III were significantly higher, the number of myocardial interstitial fibroblast cells was higher, the $+dp/dt_{max}$ and $-dp/dt_{max}$ were significantly lower, and cardiac contractility was significantly lower in the model group than control group. The accumulation of Col I/III after AMI leads to an increase in myocardial stiffness and a decline in compliance in the non-infarcted region. Meanwhile, ventricular wall thinning and expansion lead to cardiac insufficiency or heart failure.[14] The TIMP-1 molecule is a specific inhibitor of MMP-9 that can delay the degradation and remodeling of the

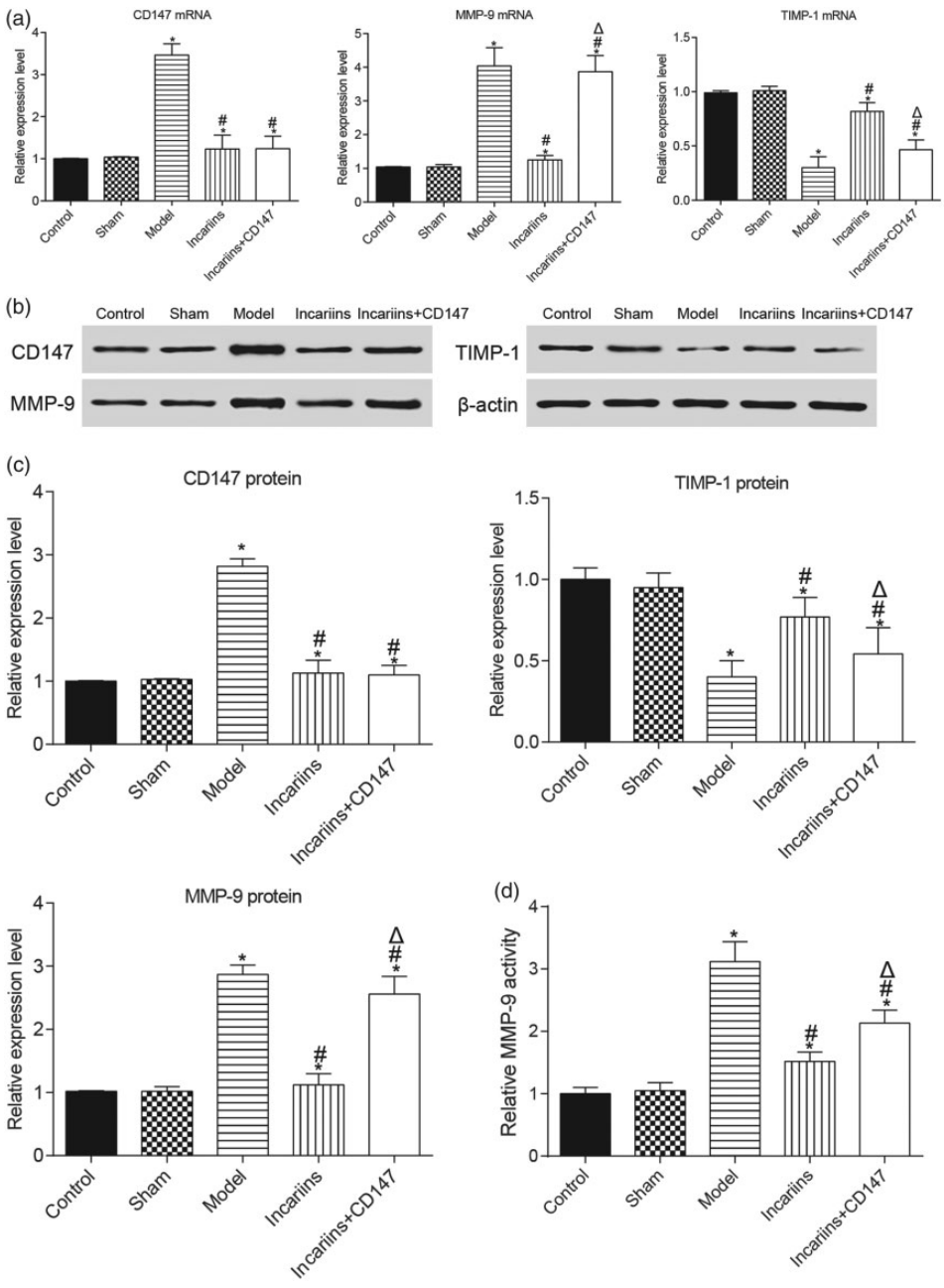

Figure 4. Expression levels of CD147, MMP-9, and TIMP-1 of rat hearts in different groups. (a) mRNA expression levels. (b) Protein expression levels. (d) Activity of MMP-9. $*P < 0.05$ compared with the control group; $\#P < 0.05$ compared with the model group; $\Delta P < 0.05$ compared with the icariin group. n = 3.

extracellular matrix.[12] In the present study, the expression level of TIMP-1 was significantly lower in the model group, and both MMP-9 and TIMP-1 were involved in cardiac remodeling following MI in rats. The expression levels of CD147 and MMP-9 were significantly lower in the icariin group than in the model group, while the expression level of TIMP was significantly higher. The icariin + CD147 group showed significant changes in the expression level of MMP-9 compared with the model group but no significant difference in the expression level of CD147 compared with the icariin group. This finding indicates that the injection of exogenous CD147 did not affect the expression level of endogenous CD147 genes but instead inhibited the expression of myocardial MMP-9, leading to the upregulation of Col I/III and blocking the inhibitive effect of icariin on cardiac remodeling.

Previous studies have shown that icariin has a protective effect on myocardial ischemia mainly by providing endothelial cell superoxide dismutase activity, reducing lipid peroxidation, and increasing the myocardial blood supply.[15] Song et al.[16] also found that icariin attenuates cardiac remodeling by downregulating myocardial apoptosis and MMP activity in congestive heart failure, proving that icariin has a positive effect on myocardial ischemia. In the present study, we detected the effect of icariin not only on MMP-9 but also on CD147. The rate of myocardial apoptosis in the icariin and icariin + CD147 groups was significantly lower than that in the model group. However, the MAP, LVEDP, $+dp/dt_{max}$, and $-dp/dt_{max}$ were significantly higher in the icariin + CD147 group than in the model group. These results demonstrate that the anti-apoptotic effects of icariin are dependent on the CD147/MMP-9 pathway on account of the improvement of the hemodynamics.[16]

In conclusion, icariin inhibited myocardial apoptosis by downregulating the CD147/MMP-9 pathway.

Declaration of conflicting interest

The authors declare that there is no conflict of interest.

Funding

This research received no specific grant from any funding agency in the public, commercial, or not-for-profit sectors.

ORCID iD

Weimin Wang http://orcid.org/0000-0002-1947-173X

References

1. Deng L, Hong T, Lin J, et al. Histamine deficiency exacerbates myocardial injury in acute myocardial infarction through impaired macrophage infiltration and increased cardiomyocyte apoptosis. *Sci Rep* 2015; 5: 13131.
2. Hassan MQ, Akhtar MS, Akhtar M, et al. Edaravone protects rats against oxidative stress and apoptosis in experimentally induced myocardial infarction: Biochemical and ultrastructural evidence. *Redox Rep* 2015; 20: 275–281.
3. Achilli F, Malafronte C, Lenatti L, et al. Granulocyte colony-stimulating factor attenuates left ventricular remodelling after acute anterior stemi: results of the single-blind, randomized, placebo-controlled multicentre stem cell mobilization in acute myocardial infarction (stem-ami) trial. *Eur J Heart Fail* 2010; 12: 1111–1121.
4. Huang L, Xu AM and Peng Q. Cd147 and mmp-9 expressions in type ii/iii adenocarcinoma of esophagogastric junction and their clinicopathological significances. *Int J Clin Exp Pathol* 2015; 8: 1929–1937.
5. Galliera E, Randelli P, Dogliotti G, et al. Matrix metalloproteases mmp-2 and mmp-9: are they early biomarkers of bone

remodelling and healing after arthroscopic acromioplasty? *Injury* 2010; 41: 1204–1207.
6. Iyer RP, Jung M and Lindsey ML. Mmp-9 signaling in the left ventricle following myocardial infarction. *Am J Physiol Heart Circ Physiol* 2016; 311: H190–H198.
7. Fu SP, Yang L, Hong H, et al. [Icariin promoted osteogenic differentiation of SD rat bone marrow mesenchymal stem cells: an experimental study]. *Zhongguo Zhong Xi Yi Jie He Za Zhi* 2015; 35: 839–846 [in Chinese, English Abstract].
8. Hu YW, Liu K and Yan MT. [Effect and mechanism of icariin on myocardial ischemia-reperfusion injury model in diabetes rats]. *Zhongguo Zhong Yao Za Zhi* 2015; 40: 4234–4239.
9. Schachinger V, Assmus B, Erbs S, et al. Intracoronary infusion of bone marrow-derived mononuclear cells abrogates adverse left ventricular remodelling post-acute myocardial infarction: insights from the reinfusion of enriched progenitor cells and infarct remodelling in acute myocardial infarction (repair-ami) trial. *Eur J Heart Fail* 2009; 11: 973–979.
10. Joubert M, Hardouin J, Legallois D, et al. Effects of glycaemic variability on cardiac remodelling after reperfused myocardial infarction: evaluation of streptozotocin-induced diabetic wistar rats using cardiac magnetic resonance imaging. *Diabetes Metab* 2016; 45: 342–350.
11. Fan X, Wu W, Shi H, et al. RNA interference targeting CD147 inhibits the invasion of human cervical squamous carcinoma cells by downregulating mmp-9. *Cell Biol Int* 2013; 37: 737–741.
12. Liu CP, Yeh JL, Wu BN, et al. Kmup-3 attenuates ventricular remodelling after myocardial infarction through enos enhancement and restoration of mmp-9/timp-1 balance. *Br J Pharmacol* 2011; 162: 126–135.
13. Zhu WH, Duan XX, Zhang MX, et al. [Evaluation of the myocardial systolic function and ventricular remodeling of rats with experimental myocardial infarction by strain/strain rate imaging and mmp-9]. *Zhonghua Xin Xue Guan Bing Za Zhi* 2010; 38: 597–600 [in Chinese, English Abstract].
14. Rouillard AD and Holmes JW. Mechanical regulation of fibroblast migration and collagen remodelling in healing myocardial infarcts. *J Physiol* 2012; 590: 4585–4602.
15. Xiang J, Zhao J, Wang Y, et al. [Effect of icariin on hypoxia/reoxygenation injury in neonatal rat cardiomyocytes]. *Zhonghua Yi Xue Za Zhi* 2015; 95: 3701–3704.
16. Song YH, Cai H, Gu N, et al. Icariin attenuates cardiac remodelling through down-regulating myocardial apoptosis and matrix metalloproteinase activity in rats with congestive heart failure. *J Pharm Pharmacol* 2011; 63: 541–549.